Magnetic Property Analysis of New Chevrel Phases

Alexis Gillette[1,2], Jessica Ortiz-Rodríguez[3], Jesús Velázquez[3], Peter Klavins[1], and Valentin Taufour[1]

[1] Department of Physics, University of California Davis, Davis, California 95616, United States of America
[2] Department of Physics, Westmont College, Santa Barbara, California 93108, United States of America
[3] Department of Chemistry, University of California Davis, Davis, California 95616, United States of America

Abstract

The magnetic properties of Chevrel phase materials synthesized via solid phase microwave synthesis were characterized. Traces of superconductivity were identified in KMo_6S_8 ($T_{c\ onset} \cong$ 3.5K) and $TiMo_6Te_8$ ($T_{c\ onset} \cong$ 2.5K). $Ni_{1.32}Mo_6Te_8$ ($\chi_0 \cong 6 \times 10^{-4}$ S.I.), $CuMo_6Te_8$ ($\chi_0 \cong 3 \times 10^{-4}$ S.I.), and $Cu_2Mo_6Te_8$ ($\chi_0 \cong 2 \times 10^{-5}$ S.I), are identified as Pauli paramagnets down to 2 K, and $NiMo_6Te_8$ exhibits paramagnetic behavior ($|\chi_0| < 10^{-5}$ S.I.). $CrMo_6Te_8$ exhibits potentially ferromagnetic behavior with a Curie temperature on the order of 300 K. In addition, an unexpectedly small signal and low temperature susceptibility curve for $ZnMo_6S_8$ uncovered Zn-leaching from the sample as discovered through re-investigating the PXRD of the sample.

1. Introduction

Chevrel Phases are a family of materials reported in 1971 by Dr. Roger Chevrel [1]. They are a group of ternary molybdenum chalcogenides of empirical formula $M_xMo_6X_8$ where M is a mono-, di-, or tri-valent metal, x is 0-4, and X is a chalcogen (S, Se, or Te). The fact that the metal may be mono-, di- or trivalent opens the door to many different possible Chevrel Phases since +1, +2, and +3 are fairly common and stable oxidation states of alkali metals, alkaline earth metals, transition metals, post-transition metals, and even the Lanthanide and Actinide series. As of 1986, there were over 100 reported Mo chalcogenides reported [2]. A diagram of the unit cell structure has been provided in Figure 1 [3]. In general, the geometry of the unit cells are usually rhombohedral (R-3) or triclinic, depending on the site preference of the cations, which in turn depends on the ionic radius and charge of the respective cation [4]

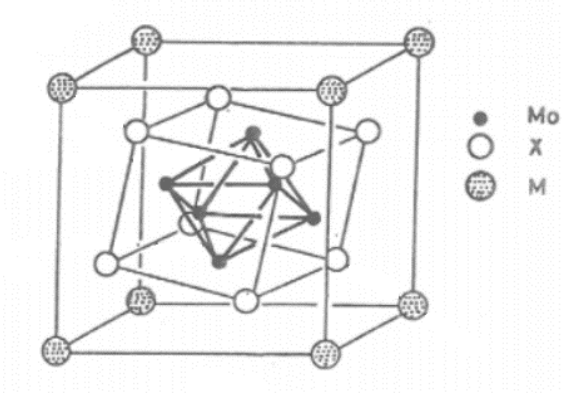

Figure 1. Unit cell structure of Chevrel Phases, stoichiometry MMo_6X_8.

By 1972, it was discovered that many Chevrel phases are superconducting, and they typically exhibit abnormally high critical fields, with $PbMo_6S_8$ having the highest critical field of up to 60 T [2,5] This value exceeds the critical field for the best binary superconductor, Nb_3Ge by over 20 T. In addition to this, $PbMo_6S_8$ also has a reported critical temperature of 14.4 K, and this is on the order of commercially used superconductors Nb_3Sn (T_c = 18 K) and NbTi (T_c = 9 K) [2]. The fact that Chevrel phases, as chalcogen-based materials, are superconductors was surprising to the scientific world of the time because until this discovery, it was thought that superconductivity was a property exclusive to “metals, alloys, or intermetallic compounds” [2]. This superconducting behavior has been attributed to the bonding present between the molybdenum clusters in the lattice, since the bonding between the Mo clusters act as “little bits of metal” so that the compounds essentially “lie at the interface between metal and molecular compounds.” In fact, this discovery opened the door to the “‘ternary-superconductors’ era” and sparked

the start of research on ternary cluster-based materials like borides, stannides, silicides, and other chalcogenides [2].

In this study, the magnetic properties of Chevrel phases synthesized via solid phase microwave synthesis are investigated with the purpose of identifying superconducting and magnetic behavior. Of the Chevrel phases investigated, $Cu_2Mo_6S_8$ (T_c = 9.15 K) and $ZnMo_6S_8$ (T_c = 2.8 K) have magnetic properties that have been previously reported, whereas KMo_6S_8, $TiMo_6Te_8$, $NiMo_6Te_8$, $Ni_{1.32}Mo_6Te_8$, $CuMo_6Te_8$, $Cu_2Mo_6Te_8$, KMo_6Te_8, and $CrMo_6Te_8$ have no previous record of being tested for magnetic properties or superconductivity [6,7].

2. Methods

2.1. Materials

The samples of each Chevrel phase were synthesized via high-temperature synthesis (>1000 ºC), medium-temperature intercalation, or room temperature intercalation by Jessica Ortiz-Rodríguez and Dr. Jesús Velázquez in the UC Davis chemistry department [4]. These samples were characterized using powder x-ray diffraction (PXRD) and energy dispersive x-ray spectroscopy (EDS) and then delivered to the UC Davis physics department for magnetic property analysis.

2.2. Sample Preparation

Each sample was prepared for analysis by placing a few milligrams of powder in a gel capsule, packing the capsule with cotton (approximately 20 mg), and then placing the capsule in a plastic straw with millimeter slits cut and folded inward to hold the capsule in place within the straw.

2.3. Magnetic Property Measurements

Magnetic property measurements were performed using a magnetic property measurement system (MPMS) with a maximum field of 7 T and a minimum temperature of 1.85 K. Scans for superconductivity were performed by applying a low field (10-100 Oe dependent upon regression fitting) and sweeping the temperature from 1.85-15 K. If the curve observed revealed a transition in M/H vs *T* curve indicating superconductivity, this was further confirmed by performing the same temperature sweep at higher fields. If no superconducting curve is observed, a temperature sweep from 2-300 K was performed at an applied field of 2 T in an effort to identify paramagnetism or other magnetic behavior. In addition to this, if the magnetization signal was on the order of 10^{-4} or lower, a background signal (obtained from running the same MPMS sequence on a system containing only a capsule, cotton, and straw) was subtracted from the overall sample signal before any further data processing or calculations.

2.4. Calculations of Magnetic Susceptibility

The data obtained from the MPMS consists of a magnetic moment (M) in emu. The volumetric magnetic susceptibility (M/H) was then calculated using the following equations:

$$\frac{M}{H} = \frac{4\pi M_{emu}}{v\mu_0 H} \times 10^{-6} \quad (1)$$

$$v = \frac{mN_A v_{uc}}{Zm_{mol}} \quad (2)$$

where $\mu_0 H$ is the applied field in Tesla, v is the volume of the sample, m is the mass of the sample, v_{uc} is the volume of the unit cell, Z is the number of formula units per unit cell, and m_{mol} is the molar mass of the compound.

3. Results and Discussion

3.1. Paramagnetic Behavior of $NiMo_6Te_8$, $Ni_{1.32}Mo_6Te_8$, $CuMo_6Te_8$, $Cu_2Mo_6Te_8$, and KMo_6Te_8

In the temperature sweep with an applied field of 2 T, $NiMo_6Te_8$, $Ni_{1.32}Mo_6Te_8$, $CuMo_6Te_8$, $Cu_2Mo_6Te_8$, and KMo_6Te_8 all provided magnetic susceptibility curves that are independent of temperature indicating

paramagnetism [Fig 2]. In addition to this, the χ_0 values listed in Table 1 are all positive, except for $NiMo_6Te_8$, indicating that $Ni_{1.32}Mo_6Te_8$, $CuMo_6Te_8$, $Cu_2Mo_6Te_8$, and KMo_6Te_8 may be classified as Pauli paramagnetic. The value of χ_0 for $NiMo_6Te_8$, however, is too small to confidently report whether it is positive and negative due to the fact that a negative background signal is of the same order of magnitude.

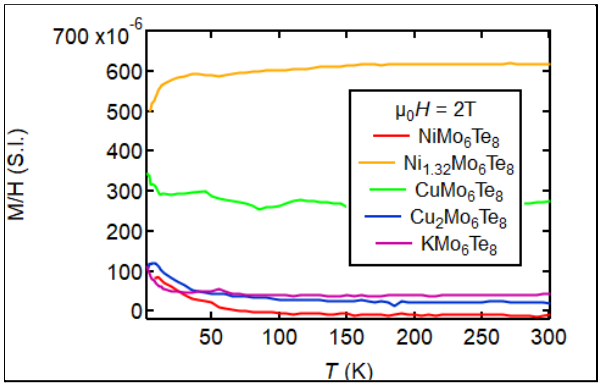

Figure 2. Magnetic susceptibility curves for the Chevrel phases identified to be paramagnetic.

Compound	Approximate χ_0
$NiMo_6Te_8$	$\lvert\chi_0\rvert < 1 \times 10^{-5}$
$Ni_{1.32}Mo_6Te_8$	6×10^{-4}
$CuMo_6Te_8$	3×10^{-4}
$Cu_2Mo_6Te_8$	2×10^{-4}
KMo_6Te_8	4×10^{-4}

Table 1. Approximate values of χ_0 for the Chevrel molybdenum tellurides identified to be paramagnetic

3.2. Superconductivity of $Cu_2Mo_6S_8$ and sample purity

$Cu_2Mo_6S_8$ is a superconductor that has previously been identified as superconducting, with a critical temperature of 9.15 K [5]. However, it was deemed beneficial to test the magnetic properties of this material to gain more insight into the quality of the samples analyzed and to check the experimental methodology being utilized in this analysis. The full susceptibility curve that is expected of a superconductor is indeed observed [Fig 3], and the transition into the superconducting state does occur around 9 K. However, the broad transition region spanning four degrees from approximately 6-10 K suggests that the sample contains impurities and/or is inhomogeneous.

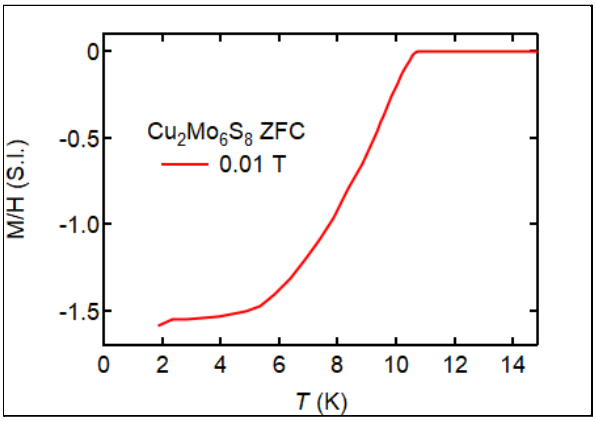

Figure 3. Magnetic susceptibility curve of $Cu_2Mo_6S_8$

The magnitude of the M/H signal of -1.5 at low temperature is lower than -1. This can be understood as a result of demagnetization effects. Indeed, the powder sample takes up a flat shape at the bottom of the capsule rather than an ideal long rod shape.

3.3. Traces of Superconductivity in KMo_6S_8 and $TiMo_6Te_8$

Traces of superconductivity were observed in both KMo_6S_8 and $TiMo_6Te_8$ with critical temperature onset values of approximately 3.5 K and 2.5 K respectively. However, full superconductivity and critical temperature values cannot be reported due to the absence of a full sharp transition in the susceptibility data. Instead, these reported critical temperature onset values were defined as the temperature at the intersection of a linear line fit to the slope of the transition region and a second linear line fit to the noise region. Despite the absence of the full superconducting transition, we confirm the presence of superconductivity within these samples due to the observed critical temperature shifts to lower temperatures as well as the decrease in amplitude as the applied magnetic field increases.

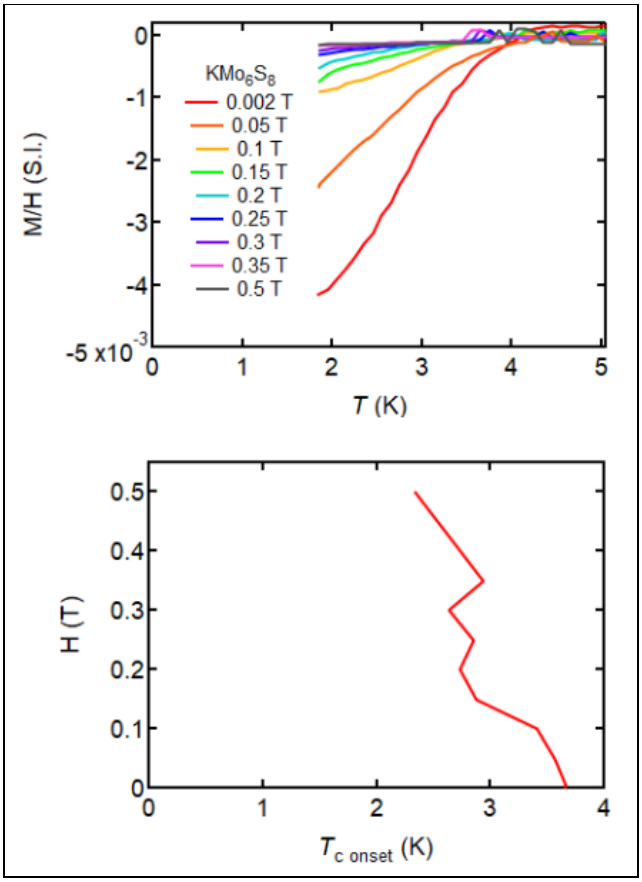

Figure 4. Magnetic susceptibility curve (top) and preliminary phase diagram (bottom) for KMo_6S_8.

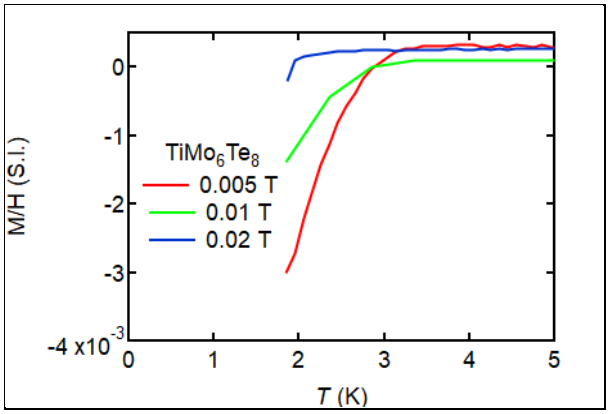

Figure 5. Magnetic susceptibility curve for $TiMo_6Te_8$.

Another reason that only traces of superconductivity may be reported is due to the small magnitude of the signals on the order of 10^{-3}, meaning that the samples are less than 0.5% superconducting. It was then postulated that an impurity may be superconducting within the sample rather than the reported species, but the PXRD data showed no impurities within the $TiMo_6Te_8$ sample and an impurity of MoS_2 within the KMo_6S_8 sample, which is only superconducting below 1.2 K and is therefore not what is giving this observed superconducting signal [8]. It is likely however, that PXRD cannot resolve an impurity of less than 0.5%.

3.4. Zn leaching from $ZnMo_6S_8$

Traces of superconductivity were also identified in the sample of $ZnMo_6S_8$, which is a known superconductor and has a reported critical temperature of 2.8 K [6]. However, the superconductivity transition observed in the magnetic susceptibility curve displayed several unexpected phenomena. The first of these is that the transition did not appear to begin until a temperature significantly lower than 2.8 K. In addition to this, the signal was again extremely small and on the order of 10^{-4}. This led to re-running the PXRD analysis of the sample, and this investigation led to the discovery that the sample had changed over time from the original synthesis and PXRD. Over time, Zn had been leaching out of the sample leaving only Mo_6S_8 (see PXRD in Figure 6). This is evidenced by the absence of peaks unique to the spectrum of $ZnMo_6S_8$ and the presence of peaks unique to Mo_6S_8 indicated in the Figure below.

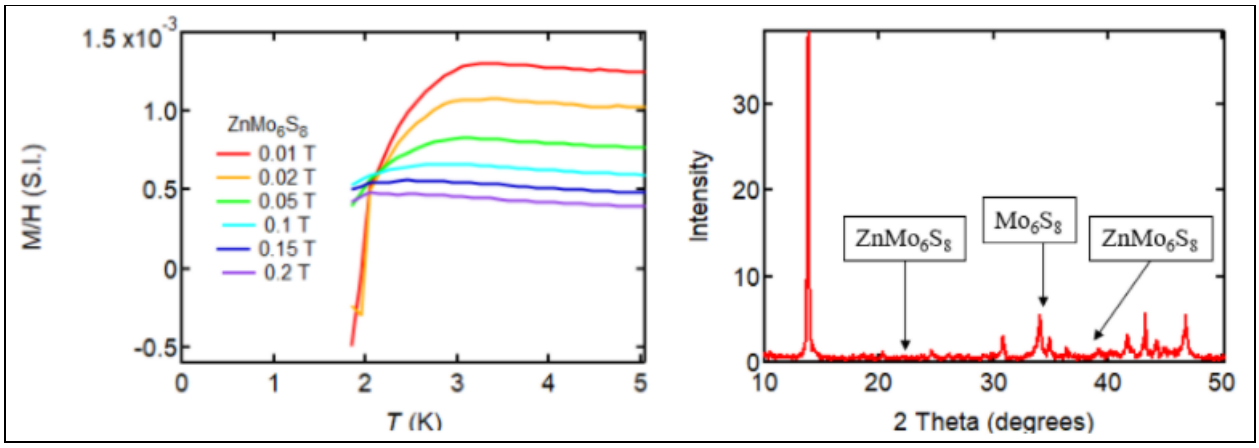

Figure 6. Magnetic susceptibility curve for sample believed to be $ZnMo_6S_8$ (left) and the PXRD (right) showing that the identity of the sample was actually Mo_6S_8 at the time of the measurement of magnetic properties.

3.5. Ferromagnetic Behavior of $CrMo_6Te_8$

The zero field-cooled magnetic susceptibility curve for $CrMo_6Te_8$ displayed what looks to be the beginning of a curve to be expected for a ferromagnet with a Curie temperature just under 300 K. Because of this, an M vs H experiment was run at temperatures 50 K (below what the susceptibility curve shows is the saturation temperature) and 300 K (near the Curie temperature). In this run, the temperature was held constant and the applied field was increased to investigate how the magnetization of the sample changes in response. The shape of the resulting M vs H curves further support the potential classification of $CrMo_6Te_8$ as a ferromagnet, though more testing is needed to confirm this claim. This is because of the small magnitude of the magnetization signal as well as the presence of an impurity of $MoTe_2$ identified in the sample's PXRD by a small peak at 12.85° adjacent to the large peak observed at 12.58° (see Figure 8). On its own, $MoTe_2$ is a semiconductor, but when it is doped with Cr, it displays ferromagnetic behavior with a T_c of around 275 K [8]. There also exist other potential impurities that may not have been evident in the PXRD that are ferromagnets with Curie temperatures around 300 K, including Cr_2Te_3 (T_c = 295 K) and more [9]. The first step in testing this possibility would be to obtain a field-cooled susceptibility curve to confirm the small value observed.

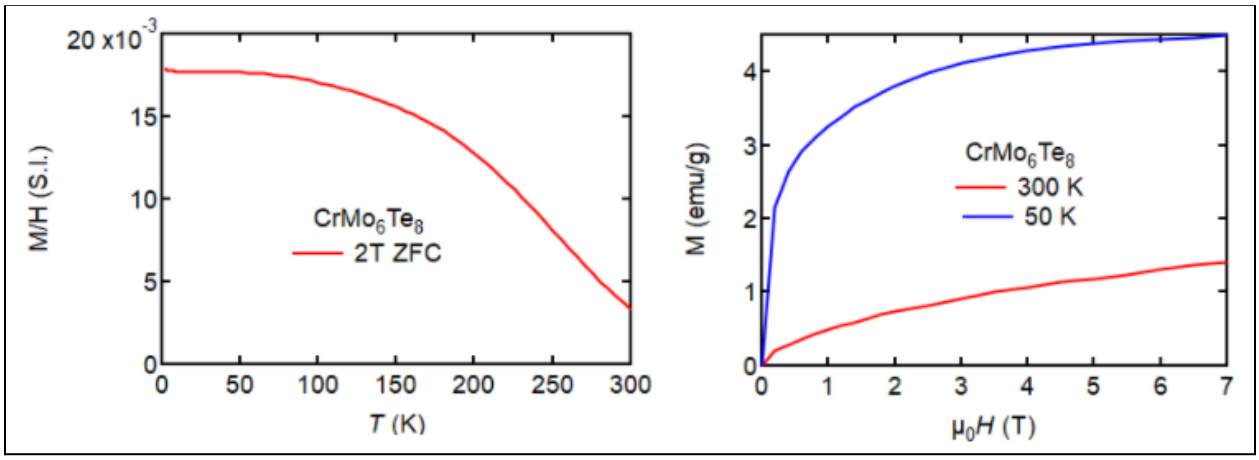

Figure 7. Magnetic susceptibility curve (left) and M vs H curves (right) for $CrMo_6Te_8$.

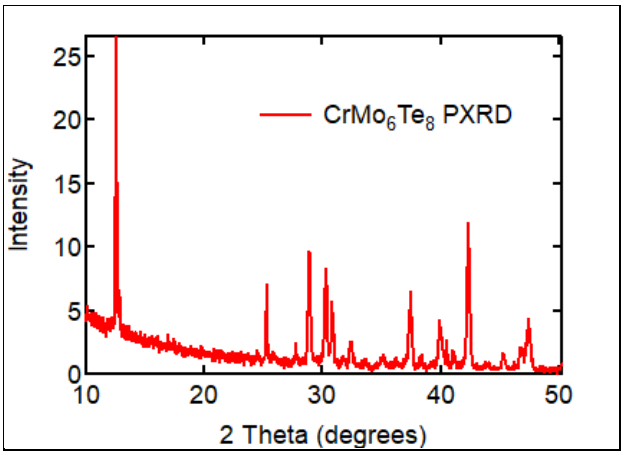

Figure 8. PXRD of $CrMo_6Te_8$ that displays evidence of an impurity of $MoTe_2$.

4. Conclusion and Future Work

In summary, we have investigated the magnetic properties of several different Chevrel phase sulfides and tellurides. In doing this, we have identified paramagnetic behaviors in $NiMo_6Te_8$, $Ni_{1.32}Mo_6Te_8$, $CuMo_6Te_8$, $Cu_2Mo_6Te_8$, and KMo_6Te_8, traces of superconductivity in KMo_6S_8 and $TiMo_6Te_8$, indications of ferromagnetic behavior in $CrMo_6Te_8$, and leaching of Zn from $ZnMo_6S_8$. Future work will be required to fully characterize the materials. The physical properties like resistivity of the superconducting materials should be tested to attempt to more accurately identify the critical temperature. PXRD and EDS data should also be obtained for $CrMo_6Te_8$ after a sample sits in an oxygenated atmosphere in an attempt to identify any impurities that may be the source of the ferromagnetic signal and rule out the existence of any species that may have arisen from oxidation or leaching. In addition to this, an hysteresis curve should also be obtained with this species to further confirm the observed ferromagnetic behavior and to identify the Curie temperature more accurately. Furthermore, the Zn-leaching from the $ZnMo_6S_8$ sample is being explored to identify the rate of the phenomenon.

5. Acknowledgements

I would like to thank Dr. Valentin Taufour and his whole research group for making this project so enjoyable and for the many things that I learned this summer. I would also like to thank Dr. Rena Zieve and Dr. Nick Curro for making the UC Davis physics REU an unforgettable experience, as well as NSF grant PHY-1852581 for the funding that made everything possible.

6. References

[1] Chevrel R, Sergent M and Prigent J. 1971 *J. Solid State Chem.* **3** 515.
[2] Chevrel R, Hirrien M and Sergent M. 1986 *Polyhedron*. **1986,** *5* 87.
[3] Peña O. 2015 *Physica C*. **514** 95.
[4] Singstock N R, Ortiz-Rogríguez J C, Perryman J T, Sutton C, Velázquez J M and Musgrave C B. 2021 *J. Am. Chem. Soc.* **143** 9113.
[5] Matthias B T, Marezio M, Corenzwit E, Cooper A S and Barz H E. 1972 *Science.* **175** 1465.
[6] Umarji A M, Subba Rao G V, Janawadkar M P and Radhakrishnan T S. 1980 *J. Phys. Chem. Solids.* **41** 421.
[7] Hohlfeld C and Pietrass B. 1982 *J. Low Temp. Phys*. **48** 503.

[8] Yang L, Hao W, Zhang L, Zahng G, Li H, Jin W, Zhang W, and Chang H. 2021 *ACS Appl. Matter Interfaces.* **13** *27* 31880.
[9] Li H, Wang L, Chen J, Yu T, Zhou L, Qiu Y, He H, Ye F, Sou I K and Wang G. 2019 *ACS Appl. Nano Mater.* **2** *11* 6809.